Mathematical Biosciences and Engineering

http://www.aimspress.com/journal/mbe

MBE, 21(3): 4648–4668.
DOI: 10.3934/mbe.2024204
Received: 19 October 2023
Revised: 19 January 2024
Accepted: 29 January 2024
Published: 29 February 2024

Research article

Stability analysis of a SAIR epidemic model on scale-free community networks

Xing Zhang, Zhitao Li and Lixin Gao*

School of Mathematics and Physics, Wenzhou University, Wenzhou 325035, China

* **Correspondence:** Email: lxgao@wzu.edu.cn.

Abstract: The presence of asymptomatic carriers, often unrecognized as infectious disease vectors, complicates epidemic management, particularly when inter-community migrations are involved. We introduced a SAIR (susceptible-asymptomatic-infected-recovered) infectious disease model within a network framework to explore the dynamics of disease transmission amid asymptomatic carriers. This model facilitated an in-depth analysis of outbreak control strategies in scenarios with active community migrations. Key contributions included determining the basic reproduction number, R_0, and analyzing two equilibrium states. Local asymptotic stability of the disease-free equilibrium is confirmed through characteristic equation analysis, while its global asymptotic stability is investigated using the decomposition theorem. Additionally, the global stability of the endemic equilibrium is established using the Lyapunov functional theory.

Keywords: SAIR; infectious disease model; network; basic reproduction number; stability

1. Introduction

With the global population continuously increasing and people's social networks expanding, the study of disease transmission has gained increasing importance. Taking COVID-19 as an example, it is evident that formulating appropriate control strategies based on the epidemic's characteristics can optimize the utilization of social resources, minimize economic losses, and reduce human casualties. In recent years, there have been significant advancements in the field of infectious disease dynamics, which have provided valuable guidance for disease transmission control and treatment. Mathematical models play a crucial role in infectious disease dynamics research by elucidating the key characteristics of diseases through assumptions, parameters, variables, and their interrelationships. Through the application of dynamic methods, mathematical models can be developed to investigate whether a specific infectious disease will continue to spread and become endemic in a particular region, or if it will eventually be eradicated.

In the realm of infectious disease modeling, compartmental models are prevalently utilized for analyzing disease spread. These models postulate that populations are divisible into homogeneous subgroups or compartments, within which individuals are indistinguishable. Parameters may vary among compartments but are constant within each one. Foundational compartmental models, such as the susceptible-infected-susceptible (SIS) and susceptible-infected-recovered (SIR) models proposed by Kermack and McKendrick [1], along with the concept of epidemic thresholds, have established a rigorous mathematical framework for the study of disease spread and the evaluation of control strategies. Progress in research has led to the introduction of additional compartments and the development of more realistic models [2–5].

The interaction between different types of networks and the dynamics of disease transmission primarily concerns how various social network structures influence the spread of diseases. For instance, scale-free networks, characterized by a few highly connected nodes, may facilitate rapid disease propagation across a large population [6–9], while small-world networks, known for short average path lengths and strong social connections, might accelerate disease spread within closely-knit groups [10–13]. These network characteristics are crucial for understanding and predicting how infectious diseases spread through populations and for formulating effective control strategies. Beyond the previously discussed models, there are also epidemic models specifically designed for overlapping community networks, as described in [14, 15]. Hence, disease models need to consider these network properties to more accurately predict and address disease transmission.

Several studies indicate that asymptomatic carriers may exhibit higher transmissibility compared to symptomatic individuals. This is attributed to asymptomatic individuals often not experiencing noticeable illness, thus possibly not undertaking necessary isolation and prevention measures. To enhance our understanding of the impact of asymptomatic carriers on disease transmission, researchers have proposed refined models, including the extensively studied SEIR model, which encompasses four states: susceptible, exposed, infectious, and recovered [16, 17]. These studies highlight the significant role of asymptomatic individuals in the dynamics of disease transmission, suggesting a need for cost-effective detection methods, such as nucleic acid testing, to inform disease control strategies. The role of asymptomatic spreaders may correlate with their social contact patterns, with skewed degree distributions indicating that some individuals, like asymptomatic carriers, have higher connectivity in social networks, potentially playing a more significant role in disease spread [18, 19].

Individual migration refers to the movement of individuals from one node to another within a network, thereby facilitating the spread of diseases across regions or communities. Such migration can be motivated by various factors, including employment, travel, or other socio-economic considerations. Incorporating individual migration in infectious disease models is crucial, as it allows diseases to traverse broader geographical or social boundaries, impacting the epidemiological dynamics across the entire network [20]. Studies, such as [21], have shown that high mobility between areas with differing infection rates significantly impacts the spread of diseases like COVID-19. Current research suggests the implementation of appropriate travel restrictions to help control the spread of diseases from high to low prevalence areas [22, 23]. Additionally, the influence of migration on disease replication and diffusion, as well as the unequal migration rates among different populations, which can substantially affect the effectiveness of control strategies, are important considerations [24].

In numerous diseases like COVID-19, asymptomatic carriers exist. While symptomatic individuals

can be isolated during epidemic management, asymptomatic carriers might spread the virus when moving to other communities. To understand their impact on disease transmission, a numerical analysis of a complex network infectious disease model across six regions was conducted, based on [25]. The study examines if a topological structure exists that minimizes active infections over time. We extend this model to a more general complex network model, incorporating asymptomatic transmission and migration features. By integrating graph theory and stability analysis, the equilibrium and stability of the nonlinear system are theoretically proven, laying a solid foundation for effective epidemic management strategies. For example, this research can inform decisions on whether it is necessary to invest a significant amount of time or resources in nucleic acid testing, by considering other studies or real-world conditions.

The key contributions of this research are threefold. First, we extend the existing model of [25] to complex networks, specifically scale-free networks, enabling a more realistic representation of disease dynamics in interconnected populations with varying degrees of connectivity. Second, we explore the stability of the nonlinear system model with asymptomatic infections on a scale-free network, substantiating the findings through rigorous theoretical proofs and simulations. Last, we investigate the dynamic behaviors of diseases in the presence of migration and assess the specific impact of unequal migration rates between different populations on disease spread.

We specifically examine the SAIR infectious disease model within a scale-free network characterized by degree correlations. We aim to explore effective strategies for controlling disease outbreaks within communities that experience migration between them. The threshold R_0, which represents the level of disease transmissibility, is determined by employing the next-generation matrix. Moreover, the global asymptotic stability of both the disease-free equilibrium and the endemic equilibrium is demonstrated through the application of the decomposition theorem [26] and the development of Lyapunov functions.

This paper is organized as follows. In Section 2, we propose an SAIR infectious disease dynamic model based on an uncorrelated network. In Section 3, we prove the existence of two equilibria of the model and calculate the basic reproduction number R_0 using the next-generation matrix method. In Section 4, we use the decomposition theorem and construct Lyapunov functions to prove the global asymptotic stability of both the disease-free equilibrium and the endemic equilibrium of the system. In Section 5, we conduct numerical simulations in MATLAB to validate the theoretical results. The paper concludes in Section 6, providing some conclusions and suggestions for future work.

2. Establishment of a SAIR network disease model

Individual migration refers to the movement of individuals from one node of the network to another, thereby facilitating the spread of diseases from one region or community to another. This type of migration can be driven by various reasons, such as employment, travel, or other socio-economic factors. In models of infectious diseases, considering individual migration is crucial as it enables diseases to transcend broader geographical or social boundaries, thereby influencing the epidemic dynamics across the entire network [20]. We employ network topology to represent the migration between individuals, assuming that within the same community, i.e., each node on the network, the total influx of different population groups, such as susceptible individuals, equals the total outflux. Infected individuals are either consciously or forcibly restricting their movements, so

there is no community migration of groups with symptomatic infections.

In the real world, social networks often exhibit the characteristics of scale-free networks, with a power-law degree distribution as their primary feature. As demonstrated in the literature [27], this common structure of social networks not only possesses the characteristic of a power-law distribution but also exhibits a dual nature of robustness and vulnerability. Furthermore, in the literature [28], an analysis of the distribution of user activities on different social media platforms reveals a similar adherence to a power-law distribution. Building upon this, We focus on the issue of epidemic spread on scale-free networks. Specifically, we extend the model proposed in the literature [25] to form model (2.1). In this model, individuals within the same node are considered to have identical characteristics, i.e., the same parameter values. Individuals within each node undergo different forms of infection processes and spread between nodes through migration at a constant rate.

Thus, this article constructs a SAIR model to describe the spread of disease within a network.

$$\begin{cases} \dot{S}_k(t) = \Lambda - \beta_k\left(\theta_k A_k(t) + I_k(t)\right) S_k(t) - \mu S_k(t) - \sigma_S S_k(t) + \sigma_S k \sum\limits_{i=1}^{n} \frac{p(i|k)}{i} S_i(t), \\ \dot{A}_k(t) = \beta_k\left(\theta_k A_k(t) + I_k(t)\right) S_k(t) - v_k A_k(t) - \mu A_k(t) - \sigma_A A_k(t) + \sigma_A k \sum\limits_{i=1}^{n} \frac{p(i|k)}{i} A_i(t), \\ \dot{I}_k(t) = v_k A_k(t) - \delta_k I_k(t) - \mu I_k(t), \\ \dot{R}_k(t) = \delta_k I_k(t) - \mu R_k(t) - \sigma_R R_k(t) + \sigma_R k \sum\limits_{i=1}^{n} \frac{p(i|k)}{i} R_i(t). \end{cases} \tag{2.1}$$

In the epidemic network we consider, each node can be in one of four different states at any time: susceptible (S), asymptomatic infected (A), symptomatic infected (I), or recovered (R). Susceptible individuals (S) can become infected by contacting symptomatic infected individuals (I) and asymptomatic infected individuals (A), with an infection rate of $\beta(\theta A + I)$, where θ represents the transmission modifying parameter for asymptomatic infected individuals (A). Only a small fraction of asymptomatic infected individuals (A) with symptoms transition to symptomatic infected individuals (I) at a rate of ν, and symptomatic infected individuals (I) recover/are removed at a rate of δ. σ_S, σ_A, and σ_R represent the migration rates of susceptible individuals (S), asymptomatic infected individuals (A), and recovered individuals (R) among different communities, respectively. The constant parameters Λ and μ represent the birth rate and natural death rate of individuals, respectively.

Due to the complexity of network structures, this article divides the nodes in the network into n classes according to their degrees, where n is the maximum degree of the network. In other words, if the degrees of nodes i and j are both k, then they belong to the kth class, where $k \in 1, 2, \cdots, n$. The state variables $S_k(t)$, $A_k(t)$, $I_k(t)$, and $R_k(t)$ represent the relative density of susceptible, asymptomatic, symptomatic, and recovered nodes with degree k. The expression $p(i|k)$ is the probability that a node with degree k is connected to a node with degree i. In an uncorrelated network, it is expressed as $p(i|k) = \frac{i}{\langle k \rangle}$ which is considered independent of the connectivity of the node that sends out the link, where $\langle k \rangle$ represents the average degree of the network.

Remark 1. *Symptomatic individuals, whether voluntarily or due to enforced restrictions, tend to restrict their activities. Consequently, there is no migration of symptomatic infection groups between communities, and migration is virtually non-existent. The social contact matrix is represented as* 0*. In contrast, asymptomatic individuals are those who have been infected with pathogens, such as viruses or bacteria, without exhibiting typical disease symptoms like fever, cough, or headache. Their clinical*

characteristics closely resemble those of susceptible and recovered individuals. Drawing inspiration from references [29, 30], we can express the social contact matrix between asymptomatic individuals, susceptible individuals, and recovered individuals as $A_{ji} = \frac{k_j k_i}{N\langle k\rangle}(i, j = 1, 2, \cdots, n)$*, where each element represents the probability of contact between individuals at node i and node j. Here,* k_i *and* k_j *represent the degrees of node i and node j, respectively. From a mean-field perspective, in the context of scale-free networks, the term for inter-community migration can be observed as the final component of model* (2.1)*. However, as asymptomatic individuals also carry the pathogen, they possess the potential to transmit the disease, akin to symptomatic individuals, through contact. The transmission probability can be represented as* $\beta_k\theta_k A_k S_k$*, where* θ_k *is a corrective parameter distinguishing it from the infection rate of symptomatic individuals. Additionally, we intend to consider adjusting parameters such as v in the future using control measures like nucleic acid testing to enhance epidemic management. Consequently, research on asymptomatic individuals carries significant importance. It is important to note that, for the sake of research convenience, this paper has not yet factored in the difference in recovery rates between asymptomatic and symptomatic individuals. Nonetheless, a more precise clinical characterization will become a crucial avenue for future research.*

Remark 2. *The model presented in this article (model* (2.1)*) has several limitations. First, although in theory, social networks can be considered scale-free networks, exhibiting power-law characteristics, many field experiments suggest that real contact networks do not follow a power-law distribution [31]. Nevertheless, scale-free networks, as a theoretical model, can effectively capture and reflect key features of real networks, such as the high concentration of connections in certain nodes. This simplification makes mathematical and computational analyses feasible, providing valuable insights for a deeper understanding of network dynamics. Second, to maintain the simplicity and ease of analysis, and since the focus of the study is on understanding long-term immune dynamics, this article omits the exposure stage by choosing to exclude the exposed category (E). It is undeniable that the exposed category (E) is crucial for the spread of the disease, and this omission represents a limitation of the model presented in this article.*

3. Boundedness of solutions and basic reproduction number

Based on Theorem 6 in the literature [26], it can be observed that the solution to model (2.1) exhibits existential uniqueness for a given initial value. Below, we present two distinct solutions to the model.

The disease-free equilibrium and endemic equilibrium are determined by solving Eq (2.1) with the right-hand side set to 0:

$$\begin{aligned}
\Lambda - \beta_k\left(\theta_k A_k(t) + I_k(t)\right) S_k(t) - \mu S_k(t) - \sigma_S S_k(t) + \sigma_S \frac{k}{\langle k\rangle}\sum_{i=1}^{n} p(i) S_i(t) = 0,\\
\beta_k\left(\theta_k A_k(t) + I_k(t)\right) S_k(t) - v_k A_k(t) - \mu A_k(t) - \sigma_A A_k(t) + \sigma_A \frac{k}{\langle k\rangle}\sum_{i=1}^{n} p(i) A_i(t) = 0,\\
v_k A_k(t) - \delta_k I_k(t) - \mu I_k(t) = 0,\\
\delta_k I_k(t) - \mu R_k(t) - \sigma_R R_k + \sigma_R(t)\frac{k}{\langle k\rangle}\sum_{i=1}^{n} p(i) R_i(t) = 0.
\end{aligned} \tag{3.1}$$

Clearly, model (2.1) possesses a disease-free equilibrium:

$$E_k^0 = (S_k^0, A_k^0, I_k^0, R_k^0) = (\frac{\Lambda}{\mu+\sigma_S} + \frac{\sigma_S}{\mu+\sigma_S}\frac{k}{<k>}\frac{\Lambda}{\mu}, 0, 0, 0).$$

To determine the endemic equilibrium, we initially manipulate Eq (3.1) to acquire:

$$\begin{aligned}
A_k^+ &= \tfrac{\delta_k+\mu}{\nu_k} I_k^+, \\
S_k^+ &= \tfrac{1}{\mu+\sigma_s}\left[\Lambda + \sigma_s \tfrac{k}{<k>} S^+ + \sigma_A \tfrac{k}{<k>} A^+ - (\nu_k + \mu + \sigma_A) A_k^+\right], \\
R_k^+ &= \tfrac{1}{\mu+\sigma_R}\left(\delta_k I_k^+ + \sigma_R \tfrac{k}{<k>} R^+\right).
\end{aligned}$$

In this context, S^+, A^+, and R^+ represent the total number (density) of susceptible individuals, asymptomatic infected individuals, and recovered individuals in each community, respectively. In other words, $S^+ = \sum_{i=1}^{n} p(i) S_i^+(t)$, $A^+ = \sum_{i=1}^{n} p(i) A_i^+(t)$, and $R^+ = \sum_{i=1}^{n} p(i) R_i^+(t)$. By substituting the above equation into the first equation of Eq (3.1), we obtain $\left(A_k^+\right)^2 + bA_k^+ + c = 0$, where $b = -\left(\Lambda + \sigma_s \frac{k}{<k>} S^+ + \sigma_A \frac{k}{<k>} A^+\right) \frac{\mu+\sigma_s}{\nu_k+\mu+\sigma_A} + \frac{(\mu+\sigma_s)(\delta_k+\mu)}{\beta_k\theta_k(\delta_k+\mu)+\beta_k\nu_k}$, $c = -\frac{\mu+\sigma_s}{\nu_k+\mu+\sigma_A}\frac{\delta_k+\mu}{\beta_k\theta_k(\delta_k+\mu)+\beta_k\nu_k}\sigma_A \frac{k}{<k>} A^+$.

Therefore, we find that $A_k^+ = \frac{-b+\sqrt{b^2-4c}}{2} > 0$. Next, we will demonstrate the positive definiteness of the local disease equilibrium.

Theorem 1. *Let* $\mathcal{D} = \left\{(S_1, A_1, I_1, R_1, \ldots, S_n, A_n, I_n, R_n) \in R_+^{4n},\ N_k(t) = S_k + A_k + I_k + R_k \le \frac{\Lambda}{\mu}\right\}$. *The set* $\mathcal{D}$ *is positively invariant for model* (2.1).

Proof. First, we illustrate the solution is positive. According to $A_k^+ > 0$, and $A_k^+ = \frac{(\delta_k+\mu)}{\nu_k} I_k^+$, we know that $I_k^+ > 0$. By weighting and summing the fourth equation of (3.1), we have $\sum_{k=1}^{n} p(k)\delta_k I_k^+(t) - \mu \sum_{k=1}^{n} p(k) R_k^+(t) = 0$, thus $R^+ > 0$ and consequently, $R_k^+ > 0$. By weighting and summing the second equation of (3.1), we have $\sum_{k=1}^{n} p(k)\beta_k(\theta_k A_k^+(t) + I_k^+(t)) S_k^+(t) - \sum_{k=1}^{n} p(k)\nu_k A_k^+(t) - \mu \sum_{k=1}^{n} p(k) A_k^+(t) = 0$. It is obvious that $\sum_{k=1}^{n} \beta_k(\theta_k A_k^+(t) + I_k^+(t)) \sum_{k=1}^{n} p(k) S_k^+(t) \ge \sum_{k=1}^{n} p(k)\beta_k(\theta_k A_k^+(t) + I_k^+(t)) S_k^+(t) > 0$, which indicates that $S^+ > 0$. Assuming that $S_k^+ < 0$, then $\forall t, \dot{S}_k > 0$, which is a contradiction. Therefore, $S_k^+ > 0$. Next, we illustrate the boundedness of the solution. The total population of each node is defined by $N_k(t) = S_k(t) + A_k(t) + I_k(t) + R_k(t)$, which satisfies $\dot{N}_k(t) = -\mu N_k(t) + \Lambda$. Obviously, we can get $N_k(t) = \left[N_k(0) - \frac{\Lambda}{\mu}\right] e^{-\mu t} + \frac{\Lambda}{\mu}$. So, we can get that $t \ge 0, N_k(t) = S_k + A_k + I_k + R_k \le \frac{\Lambda}{\mu}$.

The basic reproduction number, denoted as R_0, plays a pivotal role in epidemiology. It represents the average number of people an infected individual can transmit the disease to in the absence of any intervention measures. The computation of R_0 varies depending on the mode of disease transmission and the epidemiological model employed. Common methodologies include the next-generation matrix, epidemiological parameter estimation, branching process models, and dynamical systems analysis. The most frequently used method, particularly applicable to the compartmental models discussed in this article, is the next-generation matrix [32–35]. This approach primarily involves calculating the average number of secondary infections generated by an infective individual over the course of their infectious period. It typically requires the computation of the average expected matrix of disease transmission, followed by determining its largest eigenvalue.

According to the method of the second moment matrix, we can initially classify the districts into diseased districts $F(x)$ and non-diseased districts $V(x)$, as given by:

$$F(x) = \begin{pmatrix} \beta_k(\theta_k A_k(t) + I_k(t))S_k(t) + \sigma_A \frac{k}{<k>} \sum_{i=1}^{n} p(i)A_i(t) \\ 0 \end{pmatrix}; V(x) = \begin{pmatrix} \nu_k A_k(t) + \mu A_k(t) + \sigma_A A_k(t) \\ -\nu_k A_k(t) + \delta_k I_k(t) + \mu I_k(t) \end{pmatrix}.$$

Hence, the basic reproduction number R_0 corresponds to the largest spectral radius of the matrix FV^{-1}. In this context, F and V represent the Jacobian matrices of $F(x)$ and $V(x)$ evaluated at E_0, respectively. The matrix FV^{-1} is defined as:

$$FV^{-1} = diag\left(\frac{\beta_k \theta_k S_k^0}{\nu_k + \mu + \sigma_A} + \frac{\beta_k S_k^0 \nu_k}{(\delta_k + \mu)(\nu_k + \mu + \sigma_A)}\right) + Kdiag\left(\frac{\sigma_A}{\nu_k + \mu + \sigma_A}\right), \tag{3.2}$$

where,

$$K = \begin{bmatrix} \frac{p(1)}{\langle k \rangle} & \frac{p(2)}{\langle k \rangle} & \cdots & \frac{p(n)}{\langle k \rangle} \\ \frac{2p(1)}{\langle k \rangle} & \frac{2p(2)}{\langle k \rangle} & \cdots & \frac{2p(n)}{\langle k \rangle} \\ \vdots & \vdots & \ddots & \vdots \\ \frac{np(1)}{\langle k \rangle} & \frac{np(2)}{\langle k \rangle} & \cdots & \frac{np(n)}{\langle k \rangle} \end{bmatrix}.$$

From the above formulas, we can obtain:

1) When all parameters are the same for each community,

$$R_0 \leq \frac{\sigma_S k_{\max}}{\langle k \rangle} \frac{\beta\theta\Lambda(\delta + \mu) + \beta\Lambda\nu}{(\nu + \mu + \sigma_A)(\mu + \sigma_S)(\delta + \mu)\mu} + \frac{\beta\theta\Lambda(\delta + \mu) + \beta\Lambda\nu}{(\nu + \mu + \sigma_A)(\mu + \sigma_S)(\delta + \mu)} + \frac{\sigma_A}{\nu + \mu + \sigma_A},$$

in a finite-scale-free network with N nodes, initial node degree m_0, and adding m links at each time, the degree distribution follows $p(k) = (\gamma_1 - 1)m^{\gamma_1 - 1}k^{-\gamma_1}$. Then, $\langle k \rangle \simeq 2m$, $k_{\max} \simeq mN^{1/2}$, $R_0 < 1$, and $\sqrt{N} < \frac{2(\nu+\mu)(\mu+\sigma_S)(\delta+\mu)\mu - 2[\beta\theta\Lambda(\delta+\mu)+\beta\Lambda\nu]\mu}{[\beta\theta\Lambda(\delta+\mu)+\beta\Lambda\nu]\sigma_S}$ are equivalent;

2) When the parameters in different communities are not exactly the same,

$$R_0 = \rho\left(FV^{-1}\right) \leq \max\left(\frac{\beta_k \theta_k S_k^0}{\nu_k + \mu + \sigma_A} + \frac{\beta_k S_k^0 \nu_k}{(\delta_k + \mu)(\nu_k + \mu + \sigma_A)}\right) + \max\left(\frac{\sigma_A}{\nu_k + \mu + \sigma_A}\right).$$

The basic reproduction number R_0 is a critical metric in epidemiology, commonly used to assess the potential for the spread of infectious diseases. In epidemiology, R_0 is often compared to 1 to determine the trend of disease transmission: When $R_0 > 1$, it signifies that, on average, each infected individual can transmit the disease to more than one person. In such cases, it is expected that the disease will spread in the population and may lead to an epidemic. When $R_0 = 1$, each infected individual, on average, transmits the disease to only one other person, and the spread of the disease remains stable without expansion or reduction. When $R_0 < 1$, each infected individual, on average, transmits the disease to fewer than one person, indicating that the disease spread will gradually decline and may eventually disappear. Therefore, control measures and preventive strategies are typically designed to reduce R_0 to below 1, slowing down the spread of the disease and gaining control over the outbreak.

In situations where the network topology is uncertain, meaning the corresponding adjacency matrix is uncertain, the precise computation of the value of R_0 becomes challenging. In such cases, establishing an upper bound for R_0 is both important and meaningful. Determining an upper bound for R_0 helps us assess the potential risk of disease spread in the worst-case scenario and provides a safe threshold for epidemic control strategies. Even when the precise calculation of R_0 is not feasible, analyzing factors that may influence the upper bound of R_0 still offers valuable insights into effective epidemic control strategies.

4. Local stability and global stability of equilibria

In the context of metapopulation network models for infectious diseases, this study distinguishes between two distinct scenarios: the homogeneous case, where all communities share identical parameters, and the heterogeneous case, where parameters vary among different communities. The formulation of the upper bound for the basic reproduction number, R_0, differs under these two circumstances. It's worth noting that the homogeneous scenario essentially serves as a specific instance of the more general heterogeneous case.The analysis within this article primarily focuses on the latter, more complex scenario of heterogeneous community parameters. This approach inherently encompasses the homogeneous case, providing a comprehensive framework applicable to both specific and varied settings. Furthermore, the core of this manuscript revolves around the stability analysis of the model. It posits that if the conclusions derived for the general case (heterogeneous parameters) hold true, they will invariably apply to the special case (homogeneous parameters) as well. This methodology ensures the analysis's robustness and wide applicability, catering to a diverse range of epidemiological scenarios encountered in real-world situations.

In the following section, we will address the local stability and global stability of equilibrium points for the model under general conditions (heterogeneous parameters). The stability conclusions derived are equally applicable to the special case (homogeneous parameters). First, let's analyze the local asymptotic stability of the disease-free equilibrium point in the system.

Theorem 2. *If $R_0 < 1$, then the disease free equilibrium E_0 is locally asymptotically stable. If $R_0 > 1$, the disease free equilibrium E_0 is unstable.*

Proof. The Jacobian matrix of system (2.1) at the disease-free equilibrium E_0 is:

$$M = \begin{bmatrix} -B + \sigma_S(K-E) & -C & -D & 0 \\ 0 & C - F - B + \sigma_A(K-E) & D & 0 \\ 0 & F & -B-G & 0 \\ 0 & 0 & G & -B + \sigma_R(K-E) \end{bmatrix},$$

where, $B = diag(\mu), C = diag(\beta_k \theta_k S_k^0), D = diag(\beta_k S_k^0), F = diag(\nu_k), G = diag(\delta_k)$, because,

$$\rho(\sigma_S(K-E) - B) < \rho(-\sigma_S E - B) + \rho(\sigma_S K) = \max(-\mu) < 0,$$
$$\rho(\sigma_R(K-E) - B) < \rho(-\sigma_R E - B) + \rho(\sigma_R K) = \max(-\mu) < 0,$$

and

$$\begin{bmatrix} C - F - B + \sigma_A(K-E) & D \\ F & -B-G \end{bmatrix},$$

make a line change,we can get

$$\begin{bmatrix} C-F-B+\sigma_A(K-E)+DF(B+G) & 0 \\ F & -B-G \end{bmatrix}.$$

Obviously,

$$\begin{aligned}
&\rho(-B-G) = \max(-\mu-\delta_k) < 0;\\
&\rho(C-F-B+\sigma_A(K-E)+DF(B+G))\\
&= \rho\left(diag(\nu_k+\mu+\sigma_A)\, diag\left(\frac{\beta_k S_k^0 \nu_k}{(\delta_k+\mu)(\nu_k+\mu+\sigma_A)} + \frac{\beta_k\theta_k S_k^0-\nu_k-\mu-\sigma_A}{\nu_k+\mu+\sigma_A} + \frac{\sigma_A K}{\nu_k+\mu+\sigma_A} - 1\right)\right)\\
&\le \rho(diag(\nu_k+\mu+\sigma_A))\,\rho\left(diag\left(\frac{\beta_k S_k^0 \nu_k}{(\delta_k+\mu)(\nu_k+\mu+\sigma_A)} + \frac{\beta_k\theta_k S_k^0-\nu_k-\mu-\sigma_A}{\nu_k+\mu+\sigma_A} + \frac{\sigma_A K}{\nu_k+\mu+\sigma_A} - 1\right)\right)\\
&= \rho(diag(\nu_k+\mu+\sigma_A))\,(R_0-1) < 0.
\end{aligned}$$

The eigenvalues of M are in the left half open plane of the complex plane,so the disease free equilibrium E_0 is locally asymptotically stable.

Theorem 3. *If $R_0 < 1$, then the disease free equilibrium E^0 is globally asymptotically stable. If $R_0 > 1$, the disease free equilibrium E^0 is unstable.*

Proof. We utilize an approach from page 4 of Castillo-Chavez et al. (2002) [27] to establish the global stability of the disease-free equilibrium within the system. Within the framework of this theorem, we rewrite system (2.1) as:

$$\frac{dX}{dt} = F(X,Y),$$

$$\frac{dY}{dt} = G(X,Y), \quad with \quad G(X,0) = 0,$$

here, $X = (S_1, S_2, \cdots, S_n, R_1, R_2, \cdots, R_n) \in R_+^{2n}$ and $Y = (A_1, A_2, \cdots, A_n, I_1, I_2, \cdots, I_n) \in R_+^{2n}$ denote the dependent variables of uninfected and infected individuals, respectively. The right-hand sides, i.e., $F(X,Y)$ and $G(X,Y)$ are, respectively,

$$\begin{pmatrix}
\Lambda-\beta_1(\theta_1A_1+I_1)S_1-\mu S_1-\sigma_sS_1+\sigma_s\frac{1}{<k>}\sum_{i=1}^{n}p(i)S_i\\
\Lambda-\beta_2(\theta_2A_2+I_2)S_2-\mu S_2-\sigma_sS_2+\sigma_s\frac{2}{<k>}\sum_{i=1}^{n}p(i)S_i\\
\vdots\\
\Lambda-\beta_n(\theta_nA_n+I_n)S_n-\mu S_n-\sigma_sS_n+\sigma_s\frac{n}{<k>}\sum_{i=1}^{n}p(i)S_i\\
\delta_1I_1-\mu R_1-\sigma_RR_1+\sigma_R\frac{1}{<k>}\sum_{i=1}^{n}p(i)R_i\\
\delta_2I_2-\mu R_2-\sigma_RR_2+\sigma_R\frac{2}{<k>}\sum_{i=1}^{n}p(i)R_i\\
\vdots\\
\delta_nI_n-\mu R_n-\sigma_RR_n+\sigma_R\frac{n}{<k>}\sum_{i=1}^{n}p(i)R_i
\end{pmatrix};
\begin{pmatrix}
\beta_1(\theta_1A_1+I_1)S_1-\nu_1A_1-\mu A_1-\sigma_AA_1+\sigma_A\frac{1}{<k>}\sum_{i=1}^{n}p(i)A_i\\
\beta_2(\theta_2A_2+I_2)S_2-\nu_2A_2-\mu A_2-\sigma_AA_2+\sigma_A\frac{2}{<k>}\sum_{i=1}^{n}p(i)A_i\\
\vdots\\
\beta_n(\theta_nA_n+I_n)S_n-\nu_nA_n-\mu A_n-\sigma_AA_n+\sigma_A\frac{n}{<k>}\sum_{i=1}^{n}p(i)A_i\\
\nu_1A_1-\delta_1I_1-\mu I_1\\
\nu_2A_2-\delta_2I_2-\mu I_2\\
\vdots\\
\nu_nA_n-\delta_nI_n-\mu I_n
\end{pmatrix}.$$

According to the approach in [27], the disease-free equilibrium in this context can be expressed as:

$$E_k^0 = (X^*, 0) = (\frac{\Lambda}{\mu+\sigma_S} + \frac{\sigma_S}{\mu+\sigma_S}\frac{1}{<k>}\frac{\Lambda}{\mu}, \cdots, \frac{\Lambda}{\mu+\sigma_S} + \frac{\sigma_S}{\mu+\sigma_S}\frac{n}{<k>}\frac{\Lambda}{\mu}, 0, \cdots, 0, 0, \cdots, 0, 0, \cdots, 0),$$

is globally asymptotically stable for $R_0 < 1$ as long as the following conditions are met for (X, Y). In the first step, we understand that for the sub-system:

$$\frac{dX}{dt} = F(X,0) = \begin{pmatrix} \Lambda - \mu S_1 - \sigma_s S_1 + \sigma_s \frac{1}{<k>} \sum_{i=1}^{n} p(i) S_i \\ \Lambda - \mu S_2 - \sigma_s S_2 + \sigma_s \frac{2}{<k>} \sum_{i=1}^{n} p(i) S_i \\ \vdots \\ \Lambda - \mu S_n - \sigma_s S_n + \sigma_s \frac{n}{<k>} \sum_{i=1}^{n} p(i) S_i \\ -\mu R_1 - \sigma_R R_1 + \sigma_R \frac{1}{<k>} \sum_{i=1}^{n} p(i) R_i \\ -\mu R_2 - \sigma_R R_2 + \sigma_R \frac{2}{<k>} \sum_{i=1}^{n} p(i) R_i \\ \vdots \\ -\mu R_n - \sigma_R R_n + \sigma_R \frac{n}{<k>} \sum_{i=1}^{n} p(i) R_i \end{pmatrix},$$

the equilibrium, $X^* = (\frac{\Lambda}{\mu+\sigma_S} + \frac{\sigma_S}{\mu+\sigma_S}\frac{1}{<k>}\frac{\Lambda}{\mu}, \cdots, \frac{\Lambda}{\mu+\sigma_S} + \frac{\sigma_S}{\mu+\sigma_S}\frac{n}{<k>}\frac{\Lambda}{\mu}, 0, \cdots, 0)$, is globally asymptotically stable, which is a decoupled linear system.

Second, we observe that the Jacobian matrix given by

$$A|_{E^0} = \begin{bmatrix} A_{11} & A_{12} \\ A_{21} & A_{22} \end{bmatrix},$$

is clearly an Metzler-matrix. Here,

$$A_{11} = \begin{bmatrix} \beta_1\theta_1 - \nu_1 - \mu - \sigma_A + \sigma_A \frac{1p(1)}{<k>} & \sigma_A \frac{1p(2)}{<k>} & \cdots & \sigma_A \frac{1p(n)}{<k>}, \\ \sigma_A \frac{2p(1)}{<k>} & \beta_2\theta_2 - \nu - \mu_2 - \sigma_A + \sigma_A \frac{2p(2)}{<k>} & \cdots & \sigma_A \frac{2p(n)}{<k>} \\ \vdots & \vdots & \ddots & \vdots \\ \sigma_A \frac{np(1)}{<k>} & \sigma_A \frac{np(2)}{<k>} & \cdots & \beta_n\theta_n - \nu_n - \mu - \sigma_A + \sigma_A \frac{np(n)}{<k>} \end{bmatrix},$$

$$A_{12} = \begin{bmatrix} \beta_1 & 0 & \cdots & 0 \\ 0 & \beta_2 & \cdots & 0 \\ \vdots & \vdots & \ddots & \vdots \\ 0 & 0 & \cdots & \beta_n \end{bmatrix}, \; A_{21} = \begin{bmatrix} \nu_1 & 0 & \cdots & 0 \\ 0 & \nu_2 & \cdots & 0 \\ \vdots & \vdots & \ddots & \vdots \\ 0 & 0 & \cdots & \nu_n \end{bmatrix}, \; A_{22} = \begin{bmatrix} -\delta_1 - \mu_1 & 0 & \cdots & 0 \\ 0 & -\delta_2 - \mu_2 & \cdots & 0 \\ \vdots & \vdots & \ddots & \vdots \\ 0 & 0 & \cdots & -\delta_n - \mu_n \end{bmatrix}.$$

Then, we can get

$$
\begin{aligned}
&\widetilde{G}(X,Y) = AY - G(X,Y)\\
&= A\begin{bmatrix} A_1\\ A_2\\ \vdots\\ A_n\\ I_1\\ I_2\\ \vdots\\ I_n \end{bmatrix} - \begin{bmatrix} \beta_1(\theta_1 A_1 + I_1)S_1 - \nu_1 A_1 - \mu A_1 - \sigma_A A_1 + \sigma_A \frac{1}{<k>}\sum_{i=1}^{n} A_i\\ \beta_2(\theta_2 A_2 + I_2)S_2 - \nu_2 A_2 - \mu A_2 - \sigma_A A_2 + \sigma_A \frac{2}{<k>}\sum_{i=1}^{n} A_i\\ \vdots\\ \beta_n(\theta_n A_n + I_n)S_n - \nu_n A_n - \mu A_n - \sigma_A A_n + \sigma_A \frac{n}{<k>}\sum_{i=1}^{n} A_i\\ \nu_1 A_1 - \delta_1 I_1 - \mu I_1\\ \nu_2 A_2 - \delta_2 I_2 - \mu I_2\\ \vdots\\ \nu_n A_n - \delta_n I_n - \mu I_n \end{bmatrix} = \begin{bmatrix} \beta_1(1-S_1)(\theta_1 A_1 + I_1)\\ \beta_2(1-S_2)(\theta_2 A_2 + I_2)\\ \vdots\\ \beta_n(1-S_n)(\theta_n A_n + I_n)\\ 0\\ 0\\ \vdots\\ 0 \end{bmatrix} \geq 0.
\end{aligned}
$$

Utilizing the approach found on page 4 of [27], we can establish that the disease-free equilibrium E_0 is globally asymptotically stable.

Theorem 4. *In positive invariant $\mathcal{D}$, the endemic equilibrium E^+ of system is globally asymptotically stable, if $R_0 \geq 1$.*

Proof. Consider the Lyapunov function:

$$V_k = c_1\left(S_k - S_k^+ - S_k^+ \ln\frac{S_k}{S_k^+}\right) + c_2\left(A_k - A_k^+ - A_k^+ \ln\frac{A_k}{A_k^+}\right) + c_3\left(I_k - I_k^+ - I_k^+ \ln\frac{I_k}{I_k^+}\right),$$

with the positive coefficients c_1, c_2, c_3 satisfy $c_1 = c_2 = 1$, $c_3\nu_k A_k^+ = c_1\beta_k S_k^+ I_k^+$.

As constructed, V_k is a non-negative functional and we have

$$V_k = 0 \Leftrightarrow (S_k, A_k, I_k, R_k) = {E_k}^+.$$

Whose derivative along the solution ${E_k}^+$ gives

$$
\begin{aligned}
\dot{V}_k = {} & c_1\left(1 - \frac{S_k^+}{S_k}\right)\left[\Lambda - \beta_k(\theta A_k + I_k)S_k - \mu S_k - \sigma_S S_k + \sigma_S \frac{k}{\langle k\rangle}\sum_{i=1}^{n} p(i) S_i\right]\\
& + c_2\left(1 - \frac{A_k^+}{A_k}\right)\left[\beta_k(\theta A_k + I_k)S_k - \nu_k A_k - \mu A_k - \sigma_A A_k + \sigma_A \frac{k}{\langle k\rangle}\sum_{i=1}^{n} p(i) A_i\right]\\
& + c_3\left(1 - \frac{I_k^+}{I_k}\right)[\nu_k A_k - \delta_k I_k - \mu I_k].
\end{aligned}
$$

Since $\dot{S}_k^+ = \dot{A}_k^+ = \dot{I}_k^+ = 0$ is satisfied at ${E_k}^+$, we can get:

$$\begin{aligned}\dot{V}_k &= c_1\left(1-\frac{S_k^+}{S_k}\right)\left[\beta_k\left(\theta_k A_k^+ + I_k^+\right)S_k^+ - \beta_k\left(\theta_k A_k + I_k\right)S_k + \mu(S_k^+ - S_k) + \sigma_S(S_k^+ - S_k)\right.\\ &\left.+\sigma_S\frac{k}{\langle k\rangle}\sum_{i=1}^{n}p\left(i\right)\left(S_i - S_i^+\right)\right] + c_2\left(1-\frac{A_k^+}{A_k}\right)\left[-\beta_k\left(\theta_k A_k^+ + I_k^+\right)S_k^+ + \beta_k\left(\theta_k A_k + I_k\right)S_k\right.\\ &\left.+(\nu_k+\mu)(A_k^+ - A_k) + \sigma_A(A_k^+ - A_k) + \sigma_A\frac{k}{\langle k\rangle}\sum_{i=1}^{n}p\left(i\right)\left(A_i - A_i^+\right)\right]\\ &+ c_3\left(1-\frac{I_k^+}{I_k}\right)\left[\nu_k(A_k - A_k^+) + (\delta_k+\mu)(I_k^+ - I_k)\right]\\ &= \phi_k^1 + \phi_k^2 + \phi_k^3,\end{aligned}$$

where,

$$\begin{aligned}\phi_k^1 &= c_1\left(1-\frac{S_k^+}{S_k}\right)\left[\beta_k\left(\theta_k A_k^+ + I_k^+\right)S_k^+ - \beta_k\left(\theta_k A_k + I_k\right)S_k + \mu(S_k^+ - S_k)\right]\\ &\quad + c_2\left(1-\frac{A_k^+}{A_k}\right)\left[-\beta_k\left(\theta_k A_k^+ + I_k^+\right)S_k^+ + \beta_k\left(\theta_k A_k + I_k\right)S_k + (\nu_k+\mu)(A_k^+ - A_k)\right]\\ &\quad + c_3\left(1-\frac{I_k^+}{I_k}\right)\left[\nu_k(A_k - A_k^+) + (\delta_k+\mu)(I_k^+ - I_k)\right];\\ \phi_k^2 &= c_1\left(1-\frac{S_k^+}{S_k}\right)\left[\sigma_S(S_k^+ - S_k) + \sigma_S\frac{k}{\langle k\rangle}\sum_{i=1}^{n}p\left(i\right)\left(S_i - S_i^+\right)\right];\\ \phi_k^3 &= c_2\left(1-\frac{A_k^+}{A_k}\right)\left[\sigma_A(A_k^+ - A_k) + \sigma_A\frac{k}{\langle k\rangle}\sum_{i=1}^{n}p\left(i\right)\left(A_i - A_i^+\right)\right].\end{aligned}$$

First, simplifying ϕ_k^1, we can get:

$$\begin{aligned}\phi_k^1 &= \left(c_1\beta_k\theta_k A_k^+ S_k^+ - c_1\beta_k\theta_k A_k S_k + c_1\beta_k I_k^+ S_k^+ - c_1\beta_k I_k S_k - c_1\beta_k\theta_k A_k^+\frac{S_k^+ S_k^+}{S_k} + c_1\beta_k A_k S_k^+\right.\\ &-c_1\beta_k I_k^+\frac{S_k^+ S_k^+}{S_k} + c_1\beta_k I_k S_k^+ - c_2\beta_k\theta_k A_k^+ S_k^+ - c_2\beta_k I_k^+ S_k^+ + c_2\beta_k\theta_k A_k S_k + c_2\beta_k I_k S_k\\ &\left.+c_2\beta_k\theta_k A_k^+\frac{A_k^+ S_k^+}{A_k} + c_2\beta_k I_k^+\frac{A_k^+ S_k^+}{A_k} - c_2\beta_k\theta_k A_k^+ S_k - c_2\beta_k I_k\frac{A_k^+ S_k}{A_k} + c_1\beta_k\theta_k A_k^+ S_k^+ - c_1\beta_k\theta_k A_k^+ S_k^+\right)\\ &+ c_1\left(1-\frac{S_k^+}{S_k}\right)(\mu)(S_k^+ - S_k) + c_2\left(1-\frac{A_k^+}{A_k}\right)(\nu_k+\mu)(A_k^+ - A_k)\\ &+ c_3\left(1-\frac{I_k^+}{I_k}\right)\left[\nu_k(A_k - A_k^+) + (\delta_k+\mu)(I_k^+ - I_k)\right]\\ &= -c_1\beta_k\theta_k A_k^+ S_k^+\left(\frac{S_k}{S_k^+} + \frac{S_k^+}{S_k} - 2\right) - c_1(\mu)S_k^+\left(\frac{S_k}{S_k^+} + \frac{S_k^+}{S_k} - 2\right) + c_1\beta_k\theta_k A_k^+ S_k^+\left(\frac{A_k}{A_k^+} + \frac{A_k^+}{A_k} - 2\right)\\ &- c_2(\nu_k+\mu)A_k^+\left(\frac{A_k}{A_k^+} + \frac{A_k^+}{A_k} - 2\right) - c_3\nu_k A_k^+\left(\frac{A_k}{A_k^+} + \frac{A_k^+}{A_k} - 2\right) + c_3\nu_k A_k^+\left(\frac{A_k}{A_k^+} + \frac{A_k^+}{A_k} - 2\right)\end{aligned}$$

$$+ c_1\beta_k\left(1-\frac{S_k^+}{S_k}\right)(I_k^+S_k^+ - I_kS_k) + c_1\left(1-\frac{A_k^+}{A_k}\right)(I_kS_k - I_k^+S_k^+) + c_3\left(1-\frac{I_k^+}{I_k}\right)(\nu_kA_k - \nu_kA_k^+)$$
$$- c_3(\delta_k+\mu)I_k^+\left(\frac{I_k}{I_k^+}+\frac{I_k^+}{I_k}-2\right) = \psi_k^1+\psi_k^2+\psi_k^3,$$

with,

$$\psi_k^1 = -c_1\beta_k\theta_kA_k^+S_k^+\left(\frac{S_k}{S_k^+}+\frac{S_k^+}{S_k}-2\right) - c_1\mu S_k^+\left(\frac{S_k}{S_k^+}+\frac{S_k^+}{S_k}-2\right)$$
$$= c_1\left(-\Lambda+\beta_kI_k^+S_k^+\right)\left(\frac{S_k}{S_k^+}+\frac{S_k^+}{S_k}-2\right) + \sigma_S\left(\frac{S_k}{S_k^+}+\frac{S_k^+}{S_k}-2\right) - \sigma_S\frac{k}{\langle k\rangle}\sum_{i=1}^{n}p(i)S_i^+\left(\frac{S_k}{S_k^+}+\frac{S_k^+}{S_k}-2\right);$$
$$\psi_k^2 = c_1\beta_k\theta_kA_k^+S_k^+\left(\frac{A_k}{A_k^+}+\frac{A_k^+}{A_k}-2\right) - c_2(\nu_k+\mu)A_k^+\left(\frac{A_k}{A_k^+}+\frac{A_k^+}{A_k}-2\right) + c_3\nu_kA_k^+\left(\frac{A_k}{A_k^+}+\frac{A_k^+}{A_k}-2\right)$$
$$= \sigma_S\left(\frac{A_k}{A_k^+}+\frac{A_k^+}{A_k}-2\right) - \sigma_S\frac{k}{\langle k\rangle}\sum_{i=1}^{n}p(i)A_i^+\left(\frac{A_k}{A_k^+}+\frac{A_k^+}{A_k}-2\right);$$
$$\psi_k^3 = -c_3\nu_kA_k^+\left(\frac{A_k}{A_k^+}+\frac{A_k^+}{A_k}-2\right) + c_1\beta_k\left(1-\frac{S_k^+}{S_k}\right)(I_k^+S_k^+ - I_kS_k) + c_1\beta_k\left(1-\frac{A_k^+}{A_k}\right)(I_kS_k - I_k^+S_k^+)$$
$$+ c_3\left(1-\frac{I_k^+}{I_k}\right)(\nu_kA_k - \nu_kA_k^+) - c_3(\delta_k+\mu)I_k^+\left(\frac{I_k}{I_k^+}+\frac{I_k^+}{I_k}-2\right)$$
$$= c_1\beta_kS_k^+I_k^+\left(3-\frac{S_k^+}{S_k}-\frac{A_kI_k^+}{A_k^+I_k}-\frac{A_k^+I_kS_k}{A_kI_k^+S_k^+}\right) \le 0.$$

It is seen that $\psi_k^3 \le 0$, by virtue of the elementary inequality $(xyz)^{1/3} \le \frac{x+y+z}{3}$.

Next, we discuss those with migration items:

$$\psi_k^1+\phi_k^2 \le c_1\sigma_S\sum_{i=1}^{n}p(i)S_i^+\frac{k}{\langle k\rangle}\left(\frac{S_i}{S_i^+}-\frac{S_iS_k^+}{S_i^+S_k}-\frac{S_k}{S_k^+}+1\right),$$
$$\psi_k^2+\phi_k^3 = c_2\sigma_A\sum_{i=1}^{n}p(i)A_i^+\frac{k}{\langle k\rangle}\left(\frac{A_i}{A_i^+}-\frac{A_iA_k^+}{A_i^+A_k}-\frac{A_k}{A_k^+}+1\right).$$

Then, by virtue of the elementary inequality $1-x+\ln x \le 0, \forall x>0$. we can get that

$$\dot{V}_k = \phi_k^1+\phi_k^2+\phi_k^3 = \psi_k^1+\psi_k^2+\psi_k^3+\phi_k^2+\phi_k^3$$
$$\le \sigma_S\sum_{i=1}^{n}p(i)S_i^+\frac{k}{\langle k\rangle}\left(\frac{S_i}{S_i^+}-\frac{S_iS_k^+}{S_i^+S_k}-\frac{S_k}{S_k^+}+1\right) + \sigma_A\sum_{i=1}^{n}p(i)A_i^+\frac{k}{\langle k\rangle}\left(\frac{A_i}{A_i^+}-\frac{A_iA_k^+}{A_i^+A_k}-\frac{A_k}{A_k^+}+1\right)$$
$$\le \sigma_S\sum_{i=1}^{n}p(i)S_i^+\frac{k}{\langle k\rangle}\left(\frac{S_i}{S_i^+}+\ln\frac{S_i}{S_i^+}-\frac{S_k}{S_k^+}-\ln\frac{S_k}{S_k^+}\right) + \sigma_A\sum_{i=1}^{n}p(i)A_i^+\frac{k}{\langle k\rangle}\left(\frac{A_i}{A_i^+}+\ln\frac{A_i}{A_i^+}-\frac{A_k}{A_k^+}-\ln\frac{A_k}{A_k^+}\right).$$

Obviously, there exists a positive constant c such that

$$\sigma_A\frac{k}{\langle k\rangle}\sum_{i=1}^{n}p(i)A_i^+ = c\sigma_S\frac{k}{\langle k\rangle}\sum_{i=1}^{n}p(i)S_i^+.$$

Therefore,

$$\dot{V}_k \le \sigma_S \frac{k}{\langle k\rangle}\sum_{i=1}^{n} p(i)S_i^+\left(\frac{S_i}{S_i^+}+\ln\frac{S_i}{S_i^+}-\frac{S_k}{S_k^+}-\ln\frac{S_k^+}{S_k}+c\frac{A_i}{A_i^+}+c\ln\frac{A_i}{A_i^+}-c\frac{A_k}{A_k^+}-c\ln\frac{A_k}{A_k^+}\right)$$
$$=\sigma_S\frac{k}{\langle k\rangle}\sum_{i=1}^{n}p(i)S_i^+\left(c\frac{A_i}{A_i^+}+c\ln\frac{A_i}{A_i^+}+\frac{S_i}{S_i^+}+\ln\frac{S_i}{S_i^+}\right)-\sigma_S\frac{k}{\langle k\rangle}\sum_{i=1}^{n}p(i)S_i^+\left(c\frac{A_k}{A_k^+}+c\ln\frac{A_k}{A_k^+}\right.$$
$$\left.+\frac{S_k}{S_k^+}+\ln\frac{S_k}{S_k^+}\right)=\sigma_S\frac{k}{\langle k\rangle}\sum_{i=1}^{n}p(i)S_i^+[G_i(S_i,I_i)-G_k(S_k,I_k)],$$

where $G_i(S_i,I_i)=\left(c\frac{A_i}{A_i^+}+c\ln\frac{A_i}{A_i^+}+\frac{S_i}{S_i^+}+\ln\frac{S_i}{S_i^+}\right)$. Consider a randomly generated scale-free network graph with adjacency matrix $A=(A_{ij})_{n*n}$. The corresponding weighted directed graph is denoted as (G,A). Let $l_i=\sum_{T\in T_i}w(T)$, in which T_i is the set of all spanning trees T of (G,A) that are rooted at vertex i, and $w(T)$ is the weight of T. In particular, if (G,A) is strongly connected, then $l_i>0$ for $1\le i\le n$. and consider the corresponding weight matrix $W=(w_{ij})$ of A, where $w_{ij}=\sigma_S\frac{Aji}{k_j}S_j^+$, and k_j is the degree of node j. Then the following equation can be obtained from reference [25]:

$$\sum_{i=1}^{n}l_i\dot{V}_i=\sum_{i=1}^{n}l_i\sum_{j=1}^{n}\sigma_S\frac{A_{ji}}{k_j}S_j^+[G_j(S_j,I_j)-G_i(S_i,I_i)]=0.$$

In the context of mean-field, A_{ji} represents the probability of connection between nodes i and j. Then, by the virtue $A_{ji}=\frac{k_jk_i}{N\langle k\rangle}$, it is seen that

$$\sum_{k=1}^{n}l_k\dot{V}_k\le\sum_{k=1}^{n}l_k\sigma_S\frac{k}{\langle k\rangle}\sum_{i=1}^{n}p(i)S_i^+[G_i(S_i,I_i)-G_k(S_k,I_k)]$$
$$=\sum_{i=1}^{n}l_i\sum_{j=1}^{n}\sigma_S\frac{A_{ji}}{k_j}S_j^+\left[G_j(S_j,I_j)-G_i(S_i,I_i)\right]=0.$$

From another perspective, since we discuss scale-free networks in a mean-field sense, there is no specific form of the adjacency matrix. However, we can be certain that its result corresponds to the expectation of many specific matrices of scale-free networks. If l_i can be found for each term such that $\sum_{i=1}^{n}l_i\dot{V}i$ equals 0, then its expected form, $\sum k=1^n l_k\dot{V}_k$, must also equal 0.

From the previous context, we already know that the local disease equilibrium E^+ has a unique positive solution. By virtue of LaSalle's invariance principle, we can conclude that the disease-free equilibrium E^+ is globally asymptotically stable.

Remark 3. *In this paper, we approach the representation of scale-free networks statistically. Consequently, there is no specific matrix diagram for a scale-free network. In such cases, finding specific parameters like l_i becomes challenging. Therefore, we employ statistical concepts to demonstrate the global stability of the model's endemic equilibrium. In particular, assuming that the spanning tree weights of nodes with the same degree in a scale-free network are equal, we can select the weight of the spanning tree of nodes with the parameter l_k representing degree k to show that $\dot{V}\le 0$.*

5. Simulations

The results from the previous section indicate that when $R_0 < 1$, the disease-free equilibrium E^0 of model (2.1) is globally asymptotically stable, implying that the number of infected individuals will tend towards zero, and the disease will eventually be eradicated. Conversely, when $R_0 > 1$, the endemic equilibrium E^+ of model (2.1) is globally asymptotically stable, indicating that the number of infected individuals will tend towards a positive value I^+, and the disease will persist indefinitely. To verify the stability of the equilibria I^0 and I^+ discussed in the previous section, numerical simulations using MATLAB have been conducted in this section.

Our focus of this study is to offer a theoretical framework for analyzing and interpreting epidemic dynamics and transmission patterns under various conditions. Therefore, the parameters employed in this study, while thoughtfully constructed within the confines of a mathematical model, may not directly mirror specific biological properties. The objective of the model is to explore and comprehend the theoretical dynamics of infectious diseases and potential epidemiological patterns. This approach enables us to analyze and predict the spread of diseases on a broader and more abstract level, thus contributing to a deeper understanding of the nature of infectious disease dynamics.

To begin our exploration of the dynamics of various populations in the infectious disease model within a scale-free network, we considered the topological characteristics of such a network. Utilizing the preferential attachment algorithm, where nodes tend to connect to existing nodes with higher degrees, we devised an algorithm for the random generation of a scale-free network. This resulted in a network with a node count of $N = 1000$ and an initial network node count of $m_0 = 3$. Following the principles of the scale-free network model, $m = 2$ links were added for each new node, as illustrated in Figure 1(a). As depicted in Figure 1(b), the node distribution of this scale-free network follows a power-law form.

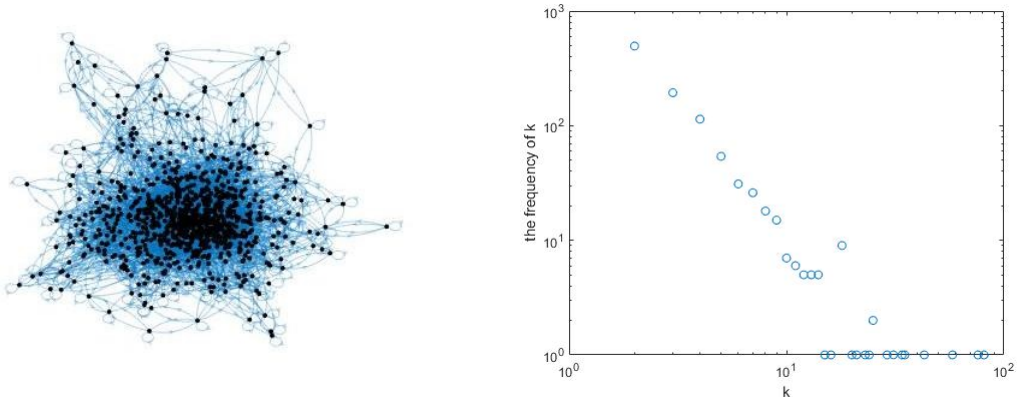

(a) Network topology illustration. **(b)** Node degree distribution statistics.

Figure 1. Scale-free graph with N =1000 nodes, $m_0 = 3$, and $m = 2$.

Second, this study places emphasis on investigating the specific impact of varying migration rates among different populations on the disease transmission capability. Accordingly, under the assumption that parameters across different compartments are equal, the dynamics of various populations within

the model have been taken into account. This approach facilitates the exploration of how differential migration rates among susceptible, infected, and recovered individuals within a community network influence the overall disease dynamics.

Select a set of parameter values: $\beta = 0.1$, $\theta = 0.02$, $\nu = 0.1$, $\delta = 0.1$, $\sigma_S = 0.01$, $\sigma_A = 0.01$, $\sigma_R = 0.01$, $\Lambda = 0.1$, $\mu = 0.1$, and initial variable values $S(0) = 0.0033$, $A(0) = 0.0033$, $I(0) = 0.0033$, $R(0) = 0$, corresponding to a basic reproduction number of $R_0 = 0.8124 < 1$.

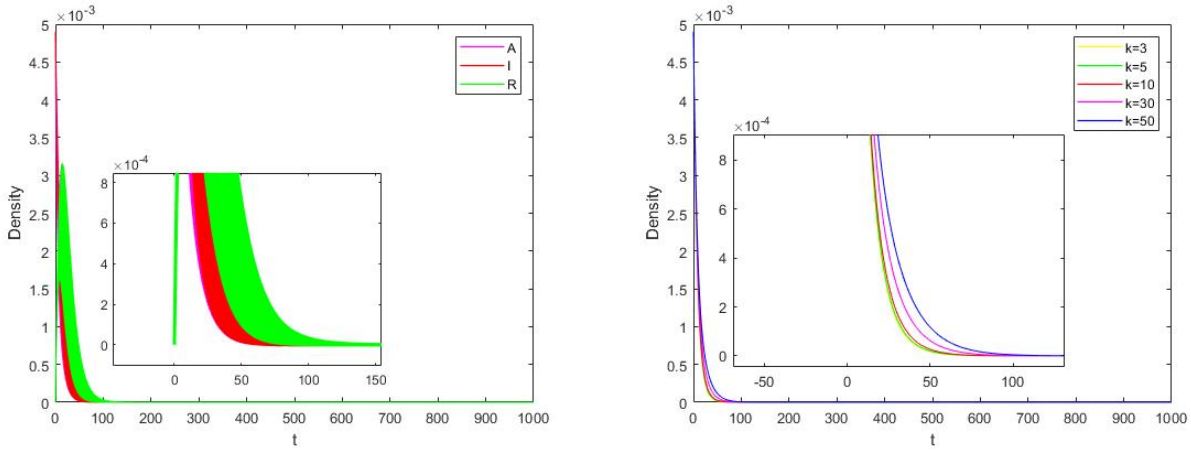

(a) Evolution trends of population densities at disease-free equilibrium.

(b) Distribution of infected population densities by degree at disease-free equilibrium.

Figure 2. Disease-free.

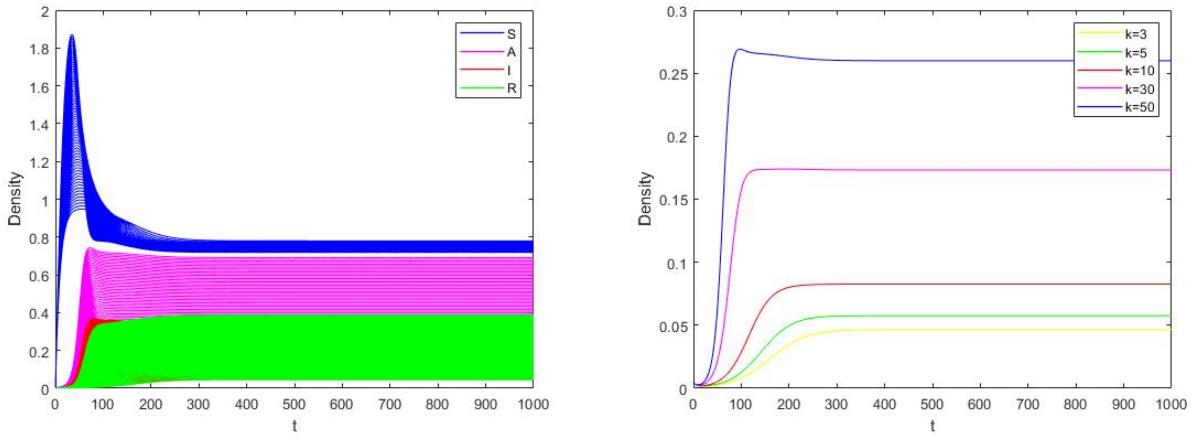

(a) Evolution trends of population densities at endemic equilibrium.

(b) Distribution of infected population densities by degree at endemic equilibrium.

Figure 3. Endemic.

From Figure 2, it can be observed that the equilibrium I is stable and tends towards I^0. Additionally, when all other parameters are held constant, the disease takes longer to disappear as k increases.

Select a set of parameter values: $\beta = 0.1$, $\theta = 0.02$, $\nu = 0.1$, $\delta = 0.1$, $\sigma_S = 0.01$, $\sigma_A = 0.01$, $\sigma_R = 0.01$, $\Lambda = 0.1$, $\mu = 0.1$, and initial variable values $S(0) = 0.0033$, $A(0) = 0.0033$, $I(0) = 0.0033$, $R(0) = 0$, corresponding to a basic reproduction number of $R_0 = 2.5235 > 1$.

From Figure 3, it is evident that the equilibrium I is stable and tends towards I^+. Additionally, when all other parameters remain constant, an increase in k leads to an increase in I^+, signifying a higher concentration of the disease.

Observations of the expressions for R_0 itself and its upper bound in Section 3 indicate that the basic reproduction number R_0 is influenced by factors such as the susceptibility migration rate and the asymptomatic migration rate. To further illustrate and discuss potential epidemic scenarios, we provide an example below.

Building upon the previous discussion, particularly from Eq (3.1), we have already established the following expressions:

In the presence of migration, we have,

$$R_0 = \rho\left(FV^{-1}\right) = \rho\left(\beta \text{diag}\left(\frac{\theta(\delta+\mu)+\nu}{(\nu+\mu+\sigma_A)(\delta+\mu)}S_k^0\right) + \frac{\sigma_A}{\nu+\mu+\sigma_A}K\right).$$

Clearly, in the absence of migration, we have,

$$R_0 = \beta\frac{\theta(\delta+\mu)+\nu}{(\nu+\mu)(\delta+\mu)}\frac{\Lambda}{\mu}.$$

It is evident from both expressions that they are related to the infection rate. To illustrate the specific impact of migration on the numerical values of R_0, taking the scale-free network illustrated in Figure 1 as an example, and we select the following parameters: $\theta = 0.02$, $\nu = 0.1$, $\delta = 0.1$, $\Lambda = 0.1$, $\mu = 0.1$, $\sigma_S = 0.1$, and $\sigma_A = 0.1$. Figure 4(a) is presented to provide an intuitive visualization of the effects of migration.

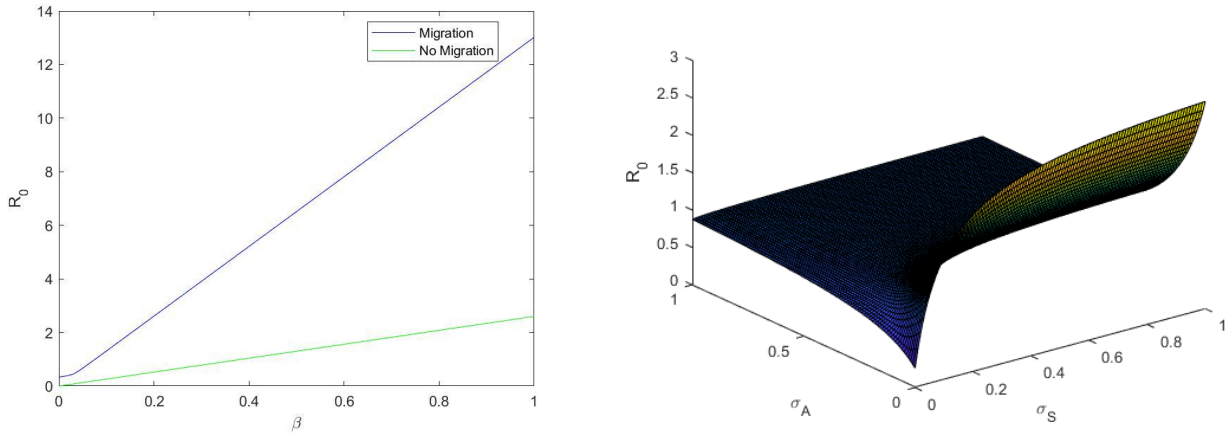

(a) Relationship between R_0 and infection rates under different migration scenarios.

(b) Correlation of R_0 with migration rates in different populations.

Figure 4. The analysis of R_0.

Next, to further investigate and demonstrate the influence of different population migration rates on R_0, we choose the parameters $\beta = 0.1$, $\theta = 0.02$, $\nu = 0.1$, $\delta = 0.1$, $\Lambda = 0.1$, and $\mu = 0.1$. This allows

us to assess the impact of susceptibility migration rate σ_S and asymptomatic infection migration rate σ_A on R_0, as shown in Figure 4(b).

From Figure 4(a), it can be observed that, consistent with the expressions for R_0, when migration is present, R_0 exhibits a nonlinear relationship with β, whereas in the absence of migration, R_0 has a linear relationship with β. Furthermore, under the same parameter conditions, when migration is present, the value of R_0 is higher than the basic reproduction number R_0 in the absence of migration. This indicates that inter-community migration makes it more challenging to eliminate infectious diseases. This result is highly reasonable because, in the presence of migration, disease transmission is not only directly related to the infection rate within the community but also influenced by the importation of cases from other communities, leading to a nonlinear relationship. In contrast, in the absence of migration, R_0 is directly related to the infection rate β. Figure 4(b) illustrates that both the susceptibility migration rate and the asymptomatic infection migration rate have an impact on the basic reproduction number R_0. Clearly, as the migration rates increase, the basic reproduction number also increases, indicating that inter-community population migration increases the likelihood of disease outbreaks. Therefore, we can conclude that the existence of migration between communities increases the probability of disease outbreaks and widens the scope of disease transmission. If not properly controlled, it may lead to widespread epidemic outbreaks.

Remark 4. *Our results illustrate that community network structure and population migration have a significant impact on the spread of infectious diseases. Notably, scale-free network structures increase the probability of disease outbreaks, and population migration expands the scope of infection. It is important to note that while the model is based on a scale-free network, the parameter values may not directly reflect biological characteristics. However, the theoretical insights provided by this study are crucial for developing effective infectious disease control strategies. Future work will explore the integration of the model with specific biological data to enhance its practical application value and biological accuracy.*

6. Conclusions

Considering the exacerbation of the epidemic due to the presence of asymptomatic individuals, especially individual migration between communities leading to widespread outbreaks, we establish a network-based SAIR infectious disease model to investigate the impact of individual migration on the spread of the disease in the presence of asymptomatic individuals. Based on this model, we calculate the epidemic threshold R_0 and find that disease transmission is not only related to intra-community parameters such as infection rate and recovery rate but is also influenced by network structure and different population migration rates between communities. Furthermore, we observe and prove, using the method of decomposition theorem and constructing a Lyapunov function, the stability of the disease-free equilibrium when $R_0 < 1$ and the stability of the endemic equilibrium when $R_0 > 1$.

Looking ahead, our objective is to enhance our model by incorporating individual connectivity differences and delving into the impact of asymptomatic carriers on disease transmission. While our current model does not differentiate individual connectivity, we acknowledge the significance of this extension. Our research agenda encompasses addressing this aspect in future studies, planning to explore more intricate network structures, and introducing additional data to better capture subtle variations in individual connectivity. This improvement will not only contribute to a more realistic

depiction of disease spread dynamics but will also extensively investigate the role of asymptomatic carriers in various connectivity scenarios. In the future, we will consider models with heterogeneous connectivity, conduct numerical tests, and comprehensively assess the influence of individual connectivity on disease dynamics. Through these efforts, we aim to deepen our understanding of disease transmission and provide valuable insights for the field of infectious disease modeling.

Use of AI tools declaration

The authors declare they have not used Artificial Intelligence (AI) tools in the creation of this article.

Acknowledgments

This work was supported by the Master's Innovation Foundation of Wenzhou University (Grant 3162023004049).

Conflict of interest

The authors declare there is no conflict of interest.

References

1. W. O. Kermack, A. G. McKendrick, Contributions to the mathematical theory of epidemics—III. Further studies of the problem of endemicity, *Bull. Math. Biol.*, **53** (1991), 89–118.
2. H. W. Hethcote, The mathematics of infectious diseases, *SIAM Rev.*, **42** (2000), 599–653. https://doi.org/10.1137/S0036144500371907
3. F. Brauer, C. Castillo-Chavez, *Mathematical Models in Population Biology and Epidemiology*, Springer, 2012.
4. Q. Lin, S. S. Musa, S. Zhao, D. He, Modeling the 2014–2015 Ebola virus disease outbreaks in Sierra Leone, Guinea, and Liberia with effect of high- and low-risk susceptible individuals, *Bull. Math. Biol.*, **82** (2020), 102. https://doi.org/10.1007/s11538-020-00779-y
5. Z. Yuan, S. S. Musa, S. Hsu, C. M. Cheung, D. He, Post pandemic fatigue: What are effective strategies, *Sci. Rep.*, **12** (2022), 9706. https://doi.org/10.1038/s41598-022-13597-0
6. S. Chen, M. Small, X. Fu, Global stability of epidemic models with imperfect vaccination and quarantine on scale-free networks, *IEEE Trans. Network Sci. Eng.*, **7** (2020), 1583–1596. https://doi.org/10.1109/TNSE.2019.2942163
7. G. Guan, Z. Guo, Bifurcation and stability of a delayed SIS epidemic model with saturated incidence and treatment rates in heterogeneous networks, *Appl. Math. Modell.*, **101** (2022), 55–75. https://doi.org/10.1016/j.apm.2021.08.024
8. R. Zhao, Q. Liu, M. Sun, Dynamical behavior of a stochastic SIQS epidemic model on scale-free networks, *J. Appl. Math. Comput.*, **68** (2022), 813–838. https://doi.org/10.1007/s12190-021-01550-9

9. Z. Xu, K. Li, M. Sun, X. Xu, Interaction between epidemic spread and collective behavior in scale-free networks with community structure, *J. Theor. Biol.*, **462** (2019), 122–133. https://doi.org/10.1016/j.jtbi.2018.11.003
10. Y. Feld, A. K. Hartmann, Large-deviations of the SIR model around the epidemic threshold, preprint, arXiv:2109.08543v2.
11. A. Dimou, M. Maragakis, P. Argyrakis, A network SIRX model for the spreading of COVID-19, *Physica A*, **590** (2022), 126746. https://doi.org/10.1016/j.physa.2021.126746
12. A. M. del Rey, R. C. Vara, S. R. González, A computational propagation model for malware based on the SIR classic model, *Neuracomputing*, **484** (2022), 161–171. https://doi.org/10.1016/j.neucom.2021.08.149
13. A. Rizzo, B. Pedalino, M. Porfiri, A network model for Ebola spreading, *J. Theor. Biol.*, **394** (2016), 212–222. https://doi.org/10.1016/j.jtbi.2016.01.015
14. Q. Yin, Z. Wang, C. Xia, C. T. Bauch, Impact of co-evolution of negative vaccine-related information, vaccination behavior and epidemic spreading in multilayer networks, *Commun. Nonlinear Sci. Numer. Simul.*, **109** (2022), 106312. https://doi.org/10.1016/j.cnsns.2022.106312
15. Y. Xue, X. Yuan, M. Liu, Global stability of a multi-group SEI model, *Appl. Math. Comput.*, **226** (2014), 51–60. https://doi.org/10.1016/j.amc.2013.09.050
16. S. Ottaviano, M. Sensi, S. Sottile, Global stability of SAIRS epidemic models, *Nonlinear Anal. Real World Appl.*, **65** (2022), 103501. https://doi.org/10.1016/j.nonrwa.2021.103501
17. A. Rahman, A. Peace, R. Kesawan, S. Ghosh, Spatio-temporal models of infectious disease with high rates of asymptomatic transmission, preprint, arXiv:2207.09671.
18. G. Dimarco, B. Perthame, G. Toscani, M. Zanella, Kinetic models for epidemic dynamics with social heterogeneity, *J. Math. Biol.*, **83** (2021), 4. https://doi.org/10.1007/s00285-021-01630-1
19. X. Liu, K. Zhao, J. Wang, H. Chen, Stability analysis of a SEIQRS epidemic model on the finite scale-free network, *Fractals*, **30** (2022), 2240054. https://doi.org/10.1142/S0218348X22400540
20. T. Das, S. R. Bandekar, A. K. Srivastav, P. K. Srivastava, M. Ghosh, Role of immigration and emigration on the spread of COVID-19 in a multipatch environment: A case study of India, *Sci. Rep.*, **13** (2023), 10546. https://doi.org/10.1038/s41598-023-37192-z
21. C. Buckee, A. Noor, L. Sattenspiel, Thinking clearly about social aspects of infectious disease transmission, *Nature*, **595** (2021), 205–213. https://doi.org/10.1038/s41586-021-03694-x
22. V. Colizzaand, A. Vespignani, Epidemic modeling in metapopulation systems with heterogeneous coupling pattern: Theory and simulations, *J. Theor. Biol.*, **251** (2008), 450–467. https://doi.org/10.1016/j.jtbi.2007.11.028
23. N. N. Wang, Y. J. Wang, S. H. Qiu, Z. R. Di, Epidemic spreading with migration in networked meta population, *Commun. Nonlinear Sci. Numer. Simul.*, **109** (2022), 106260. https://doi.org/10.1016/j.cnsns.2022.106260
24. A. R. S. Castañeda, E. E. Ramirez-Torres, L. E. Valdés-García, H. M. Morandeira-Padrón, D. S. Yanez, J. I. Montijano, et al., Model for prognostic of symptomatic, asymptomatic and hospitalized COVID-19 cases with correct demography evolution, preprint, arXiv:2206.03806v1.

25. C. J. Silva, G. Cantin, C. Cruz, R. Fonseca-Pinto, R. Passadouro, E. S. dos Santos, et al., Complex network model for COVID-19: Human behavior, pseudo-periodic solutions and multiple epidemic waves, *J. Math. Anal. Appl.*, **514** (2022), 125171. https://doi.org/10.1016/j.jmaa.2021.125171
26. M. Chapwanya, J. Lubuma, Y. Terefe, B. Tsanou, Analysis of war and conflict effect on the transmission dynamics of the tenth Ebola outbreak in the Democratic Republic of Congo, *Bull. Math. Biol.*, **84** (2022), 136. https://doi.org/10.1007/s11538-022-01094-4
27. C. Castillo-Chavez, Z. Feng, W. Huang, On the computation of R0 and its role on global stability, *Math. Approaches Emerging Re-emerging Infect. Dis. Introd.*, **125** (2002), 229–250.
28. L. Muchnik, S. Pei, L. C. Parra, S. D. S. Reis, J. S. A. Jr, S. Havlin, et al., Origins of power-law degree distribution in the heterogeneity of human activity in social networks, *Sci. Rep.*, **3** (2013), 1783. https://doi.org/10.1038/srep01783
29. M. Zanella, C. Bardelli, G. Dimarco, S. Deandrea, P. Perotti, M. Azzi, et al., A data-driven epidemic model with social structure for understanding the COVID-19 infection on a heavily affected Italian province, *Math. Models Methods Appl. Sci.*, **31** (2021), 2533–2570. https://doi.org/10.1142/S021820252150055X
30. G. Dimarco, G. Toscani, M. Zanella, Optimal control of epidemic spreading in the presence of social heterogeneity, *Phil. Trans. R. Soc. A*, **380** (2022), 20210160. https://doi.org/10.1098/rsta.2021.0160
31. G. Béraud, S. Kazmercziak, P. Beutels, D. Levy-Bruhl, X. Lenne, N. Mielcarek, et al., The French connection: The first large population-based contact survey in France relevant for the spread of infectious diseases, *PLoS One*, **10** (2015), e0133203. https://doi.org/10.1371/journal.pone.0133203
32. O. Diekmann, J. A. P. Heesterbeek, J. A. J. Metz, On the definition and the computation of the basic reproduction ratio R0 in models for infectious diseases in heterogeneous populations, *J. Math. Biol.*, **28** (1990), 365–382. https://doi.org/10.1007/BF00178324
33. R. M. Anderson, R. M. May, *Infectious Diseases of Humans: Dynamics and Control*, Oxford university press, 1991. https://doi.org/10.1017/s0950268800059896
34. H. W. Hethcote, The mathematics of infectious diseases, *SIAM Rev.*, **42** (2000), 599–653. https://doi.org/10.1137/S0036144500371907
35. P. van den Driessche, J. Watmough, Reproduction numbers and sub-threshold endemic equilibria for compartmental models of disease transmission, *Math. Biosci.*, **180** (2002), 29–48. https://doi.org/10.1016/S0025-5564(02)00108-6

AIMS Press